Comparison between a bilayer surface ordered alloy and an ideal Mn monolayer on Fe(001)

M. Taguchi, O. Elmouhssine,* C. Demangeat, and J. C. Parlebas
IPCMS-GEMM, UMR 7504 CNRS, 23, rue du Loess, F-67037 Strasbourg Cedex, France
(Received 30 March 1999)

A recent proton-induced Auger electrons experiment indicates that significant interfacial alloying occurs during the growth of the first monolayer of Mn on Fe(001). Here we report on the stability of a two-dimensional (2D) Mn-Fe surface alloy versus a perfect Mn monolayer (ML) on Fe(001). Our calculations are performed with a cell of two inequivalent atoms per plane through an *ab initio* tight-binding linear muffin-tin orbital method in the atomic-sphere approximation. A 2-ML-thick ordered $Mn_{0.5}Fe_{0.5}$ surface alloy is shown to present an antiferromagnetic configuration in the Mn sublattice. The mean magnetic moment on the Mn atoms in this 2D Mn-Fe surface alloy is shown to be higher as compared to that of a perfect Mn monolayer on Fe(001) in the antiferromagnetic $c(2\times2)$ configuration. [S0163-1829(99)04334-9]

I. INTRODUCTION

Magnetism of ultrathin metallic films on magnetic substrates is a subject of great current activity both experimentally and theoretically because of its importance in understanding the interfacial magnetism for this type of system in addition to its relevance in magnetoresistive devices. The ultrathin Mn films on Fe(001) has been one of the extensively studied systems. However, the experimental results are contradictory. On the one hand, ferromagnetic resonance measurements[1] have shown no indication of ferromagnetic order, and it was concluded that Mn on Fe(001) may be either nonmagnetic or antiferromagnetic. On the other hand, from x-ray photoelectron spectroscopy data,[2] it was concluded that each Mn atom in the Mn/Fe(001) system may have a large local magnetic moment. Magneto-optical Kerr effect (MOKE) measurements by Purcell *et al.*[3] and x-ray magnetic circular dichroism (XMCD) results by Andrieu *et al.*[4,5] have confirmed the ferromagnetic coupling between Mn atoms and a Fe substrate. Recently spin-polarized electron-energy-loss spectroscopy,[6] XMCD,[7,8] x-ray absorption, and resonant photoemission spectroscopy[9] have been performed for a monolayer (ML) and a submonolayer of Mn on Fe(001). All these experimental results show that, for a submonolayer, a large magnetic moment on each Mn atom was observed with an antiferromagnetic coupling to the Fe substrate whereas the net Mn magnetic moment vanishes for a Mn monolayer. More recently proton-induced Auger-electron spectroscopy has been performed by Igel *et al.*[10] for the topmost layer of epitaxial Mn films on Fe(100). These authors have found that significant interfacial alloying occurs during the growth of the first monolayer of Mn on Fe(100), while the second monolayer grows as a pure Mn film. Alloy formation at the interface strongly affects the magnetic ordering in ultrathin films or may even lead to a complete disappearance of the magnetic moment.

So far, theoretical investigations have been performed only for an ideal Mn monolayer or a Mn bilayer on Fe(100). Through full-potential linearized augmented-plane-wave calculations, the possibility of in-plane antiferromagnetic order has been analyzed by Wu and Freeman[11] with the $c(2\times2)$ ferrimagnetic spin configuration in Mn monolayers on Fe(001). They predicted a magnetically driven $c(2\times2)$ buckling reconstruction. Also Handschuh and Blügel[12] have found that the $c(2\times2)$ ferrimagnetic state is the stable solution for one ML of Mn on Fe(001). Within the semi-empirical tight-binding method, Vega *et al.*[13] and Pizzagalli *et al.*[14] also showed that on a Fe(001) substrate, the Mn monolayer prefers the $c(2\times2)$ ferrimagnetic configuration. Using the interface Green's-function technique based on a tight-binding linear muffin-tin orbital method, Mirbt *et al.*[15] found that the interfacial magnetic coupling between Mn and Fe changes from parallel for the monolayer to antiparallel for the bilayer, where the two Mn layers couple antiferromagnetically. However, according to Wu and Freeman,[16] this magnetic configuration for a Mn bilayer is a metastable state; they found a ground state where the magnetic moment of the surface Mn layer aligns antiparallel with that of the interfacial Mn layer and the Fe(001) substrate.

Recently, using the Korringa-Kohn-Rostoker-Green's function method, an *ab initio* study of the alloying process has been performed by Nonas *et al.*[17] in the dilute limit for 3D atoms on the Fe(001) surface. For all 3D transition-metal impurities on Fe(001) these authors found a strong tendency for a direct exchange mechanism within the first surface layer. The Mn impurities strongly repel each other on neighboring positions within the first layer.

Previously Elmouhssine *et al.*[18] investigated five possible spin configurations for the Mn monolayer on Fe(001) using a tight-binding linear muffin-tin orbital method (TB-LMTO) in the atomic-sphere approximation (ASA). They found that the two lowest configurations in energy, namely $c(2\times2)$ and $p(2\times2)\uparrow$ (the up-arrow $\uparrow$ indicates that the magnetization of the Mn layer points in the same direction as compared to the Fe substrate one) are nearly degenerate and that these two configurations lead to different interfacial magnetic couplings and mean surface magnetizations.

In this short paper we determine the stability of the bilayer surface-ordered alloy $[Mn_{0.5}Fe_{0.5}]_2/Fe(001)$ versus an ideal Mn monolayer at the surface i.e., Mn/Fe(001) using a scalar-relativistic version of the *k*-space TB-LMTO method,[19,20] within ASA. The paper is organized as follows.

TABLE I. The magnetic moments distribution of the Mn ML in the three considered magnetic configurations and for the corresponding Fe substrate layers. Fe(C) and Fe(I) represent the Fe central-layer atom and interfacial-layer atom, respectively. Data in parentheses for Fe(C) in $c(2\times2)$ state corresponds to the moment for the atom under Mn(2).

	$\mu_{Fe(C)}$	$\mu_{Fe(I-2)}$	$\mu_{Fe(I-1)}$	$\mu_{Fe(I)}$	$\mu_{Mn(1)}$	$\mu_{Mn(2)}$
$p(1\times1)\downarrow$	2.17	2.20	2.39	1.48	-3.23	-3.23
$p(1\times1)\uparrow$	2.21	2.22	2.19	1.50	3.40	3.40
$c(2\times2)$	2.15	2.19	2.34(2.23)	1.22	3.12	-3.44

The model and the formalism used in our analysis are given in Sec. II. Section III shows our calculated results. Section IV is devoted to some concluding remarks.

II. CALCULATION METHOD

Our calculations are based on the density-functional theory in the local spin-density approximation. We used the local exchange-correlation potential of von Barth and Hedin.[21] The Kohn-Sham equations are solved self-consistently in the TB-LMTO-ASA approach. In the work of Elmouhssine *et al.*[18] five possible magnetic configurations were considered for an ideal surface monolayer with four inequivalent atoms per plane. Here we add and calculate the case of a $[Mn_{0.5}Fe_{0.5}]_2/Fe(001)$-ordered surface alloy.

The Mn monolayer on the Fe(001) system is modeled by a nine-layer (001) slab consisting of a seven-layer Fe(001) film and one Mn ML on each side of the Fe film, with two inequivalent atoms per layer, hence allowing for the description of a $c(2\times2)$ structure. Two successive slabs are separated by five layers of empty spheres, using the supercell technique. This number of empty spheres is found to be sufficient to obtain well-separated noninteracting slabs,[18] thus the charge is vanishing in the central layer of the empty spheres and there is no dispersion along the *z*-axis direction. The Mn atoms are located at the ideal bcc Fe atom sites. The equilibrium lattice constant and the magnetic moments for ferromagnetic bcc Fe are found to be 5.29 a.u. and $2.16\mu_B$, respectively.[18]

The $[Mn_{0.5}Fe_{0.5}]_2/Fe(001)$ system is modeled by a nine-layer (001) slab consisting of a five-layer Fe(001) film and two ML of ordered $Mn_{0.5}Fe_{0.5}$ alloy on each side of the Fe film. Five layers of empty spheres are also used as previously considered. Both cases, i.e., Mn/Fe(001) and $[Mn_{0.5}Fe_{0.5}]_2/Fe(001)$, have the same number of Fe and Mn atoms. The distances between all layers are those of bulk Fe. We assume the magnetic coupling between Fe atoms in the alloy bilayer and Fe(001) substrate to be parallel. Within these assumptions, all magnetic calculations are performed. In order to make a reliable comparison between the total energies of all these configurations, we choose the same unit cell [$c(2\times2)$ unit cell] and the same number of *k* points in the irreducible Brillouin zone (BZ). For the *k*-space integration we used the tetrahedron method[22,23] and an increasing number of *k* points, until final convergence was obtained for 847 *k* points in the irreducible BZ.

III. RESULTS AND DISCUSSION

The local magnetic moments of $c(2\times2)$, $p(1\times1)\uparrow$, and $p(1\times1)\downarrow$ magnetic configurations for one Mn monolayer on Fe(001) are shown in Table I. The local magnetic moments of the $[Mn_{0.5}Fe_{0.5}]_2$ bilayer on Fe(001) are shown in Table II. As we mentioned in Sec. II, we modeled the system by a 2-ML-thick ordered 2D alloy with $Mn_{0.5}Fe_{0.5}$ composition per ML. In this case, by considering two inequivalent atoms per plane within two surface planes we had to start, in principle, with 2^4 magnetic configurations as input parameters in order to be very general. However, we restricted ourselves to solutions with all the Fe atoms ferromagnetically aligned. Only Mn atoms were expected to be ferromagnetically or antiferromagnetically coupled to Fe atoms so that we remained with four configurations as input parameters as shown in Fig. 1, i.e., (i) Mn(S)$\uparrow$ and Mn(S-1)$\uparrow$ (alloy I); (ii) Mn(S)$\downarrow$, and Mn(S-1)$\uparrow$ (alloy II); (iii) Mn(S)$\uparrow$ and Mn(S-1)$\downarrow$ (alloy III); and (iv) Mn(S)$\downarrow$ and Mn(S-1)$\downarrow$ (alloy IV). X(S) and X(S-1)(X=Mn, Fe) represent the X surface-layer and subsurface-layer atom, respectively. The Fe substrate determines the orientation of the Mn(S-1) magnetic moments. Only magnetic configuration with ferromagnetic coupling between Fe substrate and Mn(S-1) survive after self-consistency. Therefore, alloy III and alloy IV magnetic configurations with antiferromagnetic coupling between Mn(S-1) and Fe(S-1) atoms converge, respectively, towards alloy I and alloy II with ferromagnetic coupling between Mn(S-1) and Fe(S-1) atoms. For the alloy II configuration, the magnetic moments of the subsurface-layer Fe(S-1) and Mn(S-1) atoms are substantially diminished to only 1.5 and $1.2\mu_B$. This decrease of the magnetic moments at the subsurface layer can be seen in the case of Mn bilayer on Fe(001) systems.[15,16] On the other hand, due to the band narrowing at the surface layer by reducing the coordination number, the magnetic moments of Fe(S) at the surface layer ($2.6\mu_B$) is substantially enhanced with respect to the moment in the corresponding bulk Fe of $2.16\mu_B$. For alloy I

TABLE II. The magnetic moment distribution of the atoms in a 2-ML-thick and ordered alloy $[Mn_{0.5}Fe_{0.5}]_2/Fe(001)$ atoms for the two converged magnetic configurations (Fig. 1) and for the corresponding Fe substrate layers. Fe(C) represents the Fe central-layer atom. Mn(S) and Fe(S) label the Mn and Fe surface-layer atom, respectively. Mn(S-1) and Fe(S-1) represent the Mn and Fe subsurface-layer atom, respectively. Data in parentheses for Fe(C) and Fe(I-1) correspond to the moment for the atom under Mn(S). Data in parentheses for Fe(I-2) correspond to the moment for the atom under Fe(S-1).

	$\mu_{Fe(C)}$	$\mu_{Fe(I-2)}$	$\mu_{Fe(I-1)}$	$\mu_{Fe(S-1)}$	$\mu_{Mn(S-1)}$	$\mu_{Fe(S)}$	$\mu_{Mn(S)}$
Alloy I	2.21(2.24)	2.25(2.28)	2.10(2.05)	1.72	0.31	2.75	3.25
Alloy II	2.13(2.21)	2.23(2.21)	2.18(2.15)	1.50	1.20	2.60	-3.33

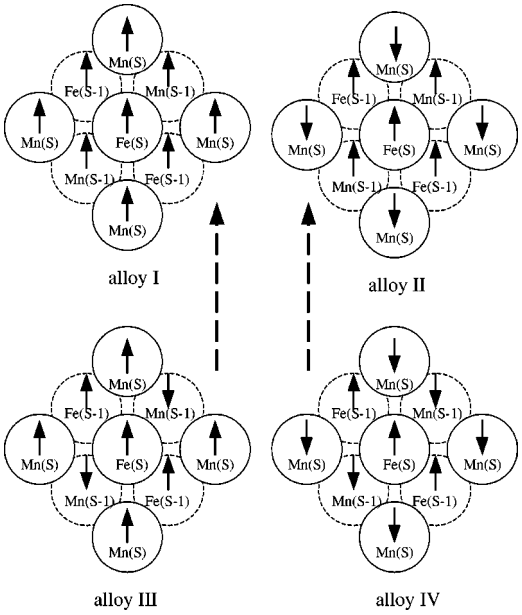

FIG. 1. Schematic representation of the four investigated magnetic configurations for a $[Mn_{0.5}Fe_{0.5}]_2$ bilayer on Fe(001). Solid (dashed) circles correspond to the surface Mn and Fe atoms (subsurface Mn and Fe atoms). The arrows indicate the direction of the moments. X(S) and X(S-1) (X=Mn, Fe) represent the X surface-layer and subsurface-layer atom, respectively. Alloy III and alloy IV configurations converge towards alloy I and alloy II configurations, respectively.

configuration, the magnetic moments of the subsurface-layer Fe(S-1) and Mn(S-1) atoms also diminished; especially the magnetic moments of subsurface-layer Mn(S-1) atom are very small ($0.3\mu_B$). Figure 2 reports the relative energies of the $p(1\times1)\downarrow$, alloy II, $p(1\times1)\uparrow$ and alloy I versus the $c(2\times2)$ ground-state energy. The $p(1\times1)\uparrow$ and $p(1\times1)\downarrow$ configurations are, respectively, about 81 and 232 meV higher in energy with respect to the $c(2\times2)$ one, in good agreement with previous theoretical results.[12] Figure 2 displays clearly that $c(2\times2)$ and alloy II are almost degenerate in energy. The alloy II configuration is only 7 meV above the $c(2\times2)$ one. This means that in experiment at room temperature the magnetic structure may be modified by subtle differ-

ences of temperature (300 $K\equiv25$ meV) and relaxation (~10 meV).[12] Both alloy II and $c(2\times2)$ configurations have the same magnetic profile, i.e., in-plane antiferromagnetic order at the surface layer [between Mn and Fe atoms for alloy II and between Mn atoms for $c(2\times2)$] and in-plane ferromagnetic order at the sublayer [between Mn and Fe atoms for alloy II and between Fe atoms for $c(2\times2)$]. Moreover, in both cases the magnetic moments of the Mn atoms at nearest neighboring positions (alloy II) and next nearest neighboring position $[c(2\times2)]$ are coupled antiferromagnetically. Purely ferromagnetic configurations for Mn atoms are unlikely.

In order to investigate the effect of the formation of local magnetic moments, we calculate also the total energy of the $[Mn_{0.5}Fe_{0.5}]_2$ bilayer on Fe(001) and one Mn ML on Fe(001) systems for the nonmagnetic solution. Our results reveal that, for the nonmagnetic solution, the $[Mn_{0.5}Fe_{0.5}]_2$ bilayer on Fe(001) is more stable than the one Mn ML on Fe(001) by

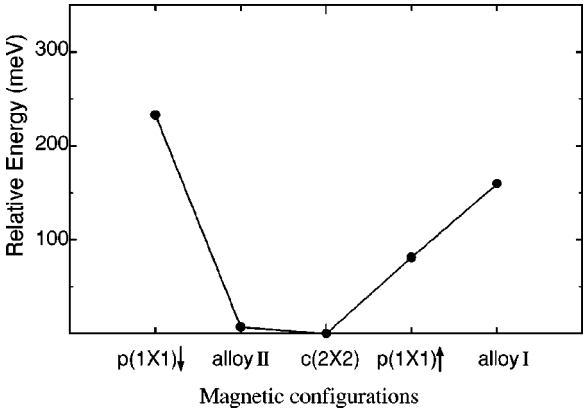

FIG. 2. Relative energy $E-E_{c(2\times2)}$ for five magnetic configurations in units of meV. The zero energy corresponds to the $c(2\times2)$ state. The small energy difference between $c(2\times2)$ and alloy II configurations indicates that the two solutions are nearly degenerate ground states.

100 meV whereas, as we mentioned before, $c(2\times2)$ magnetic configuration is more stable than alloy II one. A similar result has been obtained recently by Blügel[24] in the case of Mn MLs on Cu(001). This clearly shows that magnetism is very important in order to stabilize the $c(2\times2)$ magnetic configuration.

IV. CONCLUDING REMARKS

In this paper, following the paper of Igel *et al.*,[10] we discussed the stability of a 2D Mn-Fe ordered surface alloy with a 2 ML thickness on Fe(001) substrate. Alloy II with Mn(S)$\downarrow$ and Mn(S-1)$\uparrow$ was shown to be the ground state of the alloyed configurations. Its energy was found to be only 7 meV above the $c(2\times2)$ ground state obtained for one Mn ML on Fe(001). Therefore, it is expected that alloying between Mn and Fe will be present at the Mn-Fe interface in agreement with Igel *et al.*[10] However, from a mean surface magnetization point of view there is a big difference between both nearly degenerate ground states. For the $c(2\times2)$ configuration the mean magnetic moment of the Mn atoms is shown to be as small as $0.16\mu_B$ whereas it is $1.07\mu_B$ for the alloy II configuration. Therefore, we suggest that very precise XMCD and MOKE experiments might be able to discriminate between them. From our calculation for $[Mn_{0.5}Fe_{0.5}]_2$ bilayer on Fe(001), we obtained a ground-state magnetic configuration with antiferromagnetic coupling between Mn atoms at nearest-neighboring positions. This antiferromagnetic coupling has been obtained by other authors.[25] Therefore, we believe that this antiferromagnetic coupling will remain true when changing the alloy composition.

ACKNOWLEDGMENTS

M. Taguchi gratefully acknowledges financial support from the Canon Foundation. Also O. Elmouhssine would like to acknowlege partial support from the European TMR ''Interface Magnetism.''

*Present address: BUGH Wuppertal, FB-9 Theor. Chem., Gauss Strasse 20, D-42097 Wuppertal, Germany.

[1] B. Heinrich, A. S. Arrot, J. F. Cochran, C. Liu, and K. Myrtle, J. Vac. Sci. Technol. A **4**, 1376 (1986).
[2] B. Heinrich, A. S. Arrot, C. Liu, and S. T. Purcell, J. Vac. Sci. Technol. A **5**, 1935 (1987).
[3] S. T. Purcell, M. T. Johnson, N. W. McGee, R. Coehoorn, and W. Hoving, Phys. Rev. B **45**, 13 064 (1992).
[4] S. Andrieu, M. Finazzi, F. Yubero, H. Fischer, P. Arcade, F. Chevrier, K. Hricovini, G. Krill, and M. Piecuch, J. Magn. Magn. Mater. **165**, 191 (1997).
[5] S. Andrieu, M. Finazzi, F. Yubero, H. M. Fischer, Ph. Arcade, F. Chevrier, L. Hennet, K. Hricovini, G. Krill, and M. Piecuch, Europhys. Lett. **38**, 459 (1997).
[6] Ch. Roth, Th. Kleeman, F. U. Hillebrecht, and E. Kisker, Phys. Rev. B **52**, R15 691 (1995).
[7] O. Rader, W. Gudat, D. Schmitz, C. Carbone, and W. Eberhardt, Phys. Rev. B **56**, 5053 (1997).
[8] J. Dresselhaus, D. Spanke, F. U. Hillebrecht, E. Kisker, G. van der Laan, J. B. Goedkoop, and N. B. Brookes, Phys. Rev. B **56**, 5461 (1997).
[9] H. A. Dürr, G. van der Laan, D. Spanke, F. U. Hillebrecht, and N. B. Brooks, Phys. Rev. B **56**, 8156 (1997).
[10] T. Igel, R. Pfandzelter, and H. Winter, Surf. Sci. **405**, 182 (1998).
[11] R. Wu and A. J. Freeman, Phys. Rev. B **51**, 17 131 (1995).
[12] S. Handschuh and S. Brügel, Solid State Commun. **105**, 633 (1998).
[13] A. Vega, S. Bouarab, H. Dreyssé, and C. Demangeat, Thin Solid Films **275**, 103 (1996).
[14] L. Pizzagalli, D. Stoeffler, and F. Gautier, Phys. Rev. B **54**, 12 216 (1996).
[15] S. Mirbt, O. Eriksson, B. Johansson, and H. L. Skriver, Phys. Rev. B **52**, 15 070 (1995).
[16] R. Wu and A. J. Freeman, J. Magn. Magn. Mater. **161**, 89 (1996).
[17] B. Nonas, K. Wildberger, R. Zeller, and P. H. Dederichs, Phys. Rev. Lett. **80**, 4574 (1998).
[18] O. Elmouhssine, G. Moraïtis, C. Demangeat, and J. C. Parlebas, Phys. Rev. B **55**, R7410 (1997).
[19] O. K. Andersen and O. Jepsen, Phys. Rev. Lett. **53**, 2571 (1984).
[20] O. K. Andersen, Z. Pawlowska, and O. Jepsen, Phys. Rev. B **34**, 5253 (1986).
[21] U. von Barth and X. Hedin, J. Phys. C **5**, 1629 (1972).
[22] O. Jepsen and O. K. Andersen, Solid State Commun. **9**, 1763 (1971).
[23] G. Lehman and M. Taut, Phys. Status Solidi B **54**, 469 (1972).
[24] S. Blügel, Appl. Phys. A: Mater. Sci. Process. **63**, 595 (1996).
[25] S. Meza-Aguilar, O. Elmouhssine, H. Dreyssé, and C. Demangeat (unpublished).